EUROPEAN UROLOGY XXX (2016) XXX–XXX

available at www.sciencedirect.com
journal homepage: www.europeanurology.com

European Association of Urology

Platinum Priority – Prostate Cancer
Editorial by XXX on pp. x–y of this issue

Subgroups of Castration-resistant Prostate Cancer Bone Metastases Defined Through an Inverse Relationship Between Androgen Receptor Activity and Immune Response

Erik Bovinder Ylitalo [a], *Elin Thysell* [a], *Emma Jernberg* [a], *Marie Lundholm* [a], *Sead Crnalic* [b], *Lars Egevad* [c], *Pär Stattin* [d], *Anders Widmark* [e], *Anders Bergh* [a], *Pernilla Wikström* [a,*]

[a] *Department of Medical Biosciences, Pathology, Umea University, Umea, Sweden;* [b] *Department of Surgery and Perioperative Sciences, Orthopedics, Umea University, Umea, Sweden;* [c] *Section of Urology, Department of Surgical Science, Karolinska Institutet, Stockholm, Sweden;* [d] *Department of Surgery and Perioperative Sciences, Urology & Andrology, Umea University, Umea, Sweden;* [e] *Department of Radiation Sciences, Oncology, Umea University, Umea, Sweden*

Article info

Article history:
Accepted July 19, 2016

Associate Editor:
Giacomo Novara

Keywords:
Bone metastasis
Castration-resistance
Immune response
Metabolism
Prostate cancer

Abstract

Background: Novel therapies for men with castration-resistant prostate cancer (CRPC) are needed, particularly for cancers not driven by androgen receptor (AR) activation.
Objectives: To identify molecular subgroups of PC bone metastases of relevance for therapy.
Design, setting, and participants: Fresh-frozen bone metastasis samples from men with CRPC ($n = 40$), treatment-naïve PC ($n = 8$), or other malignancies ($n = 12$) were characterized using whole-genome expression profiling, multivariate principal component analysis (PCA), and functional enrichment analysis. Expression profiles were verified by reverse transcription–polymerase chain reaction (RT-PCR) in an extended set of bone metastases ($n = 77$) and compared to levels in malignant and adjacent benign prostate tissue from patients with localized disease ($n = 12$). Selected proteins were evaluated using immunohistochemistry. A cohort of PC patients ($n = 284$) diagnosed at transurethral resection with long follow-up was used for prognostic evaluation.
Results and limitations: The majority of CRPC bone metastases (80%) was defined as AR-driven based on PCA analysis and high expression of the AR, AR co-regulators (FOXA1, HOXB13), and AR-regulated genes (*KLK2*, *KLK3*, *NKX3.1*, *STEAP2*, *TMPRSS2*); 20% were non–AR-driven. Functional enrichment analysis indicated high metabolic activity and low immune responses in AR-driven metastases. Accordingly, infiltration of $CD3^+$ and $CD68^+$ cells was lower in AR-driven than in non–AR-driven metastases, and tumor cell HLA class I ABC immunoreactivity was inversely correlated with nuclear AR immunoreactivity. RT-PCR analysis showed low MHC class I expression (*HLA-A*, *TAP1*, and *PSMB9* mRNA) in PC bone metastases compared to benign and malignant prostate tissue and bone metastases of other origins. In primary PC, low HLA class I ABC immunoreactivity was associated with high Gleason score, bone metastasis, and short cancer-specific survival. Limitations include the limited number of patients studied and the single metastasis sample studied per patient.
Conclusions: Most CRPC bone metastases show high AR and metabolic activities and low immune responses. A subgroup instead shows low AR and metabolic activities, but high immune responses. Targeted therapy for these groups should be explored.

* Corresponding author. Department of Medical Biosciences, Umeå University, 901 85 Umeå, Sweden. Tel. +46 90 7853752; Fax: +46 90 7852829.
E-mail address: pernilla.wikstrom@umu.se (P. Wikström).

http://dx.doi.org/10.1016/j.eururo.2016.07.033

Please cite this article in press as: Ylitalo EB, et al. Subgroups of Castration-resistant Prostate Cancer Bone Metastases Defined Through an Inverse Relationship Between Androgen Receptor Activity and Immune Response. Eur Urol (2016), http://dx.doi.org/10.1016/j.eururo.2016.07.033

Patient summary: We studied heterogeneities at a molecular level in bone metastasis samples obtained from men with castration-resistant prostate cancer. We found differences of possible importance for therapy selection in individual patients.

1. Introduction

The growth of normal and malignant prostate tissue is regulated by androgens through activation of the androgen receptor (AR) in both epithelial and stromal cells, and androgen deprivation therapy (ADT) is standard treatment for patients with advanced prostate cancer (PC). However, after an initial period of reduced symptoms and tumor growth, relapse occurs and the PC becomes castration resistant (CRPC). Several mechanisms behind CRPC have been described, including AR amplification, AR mutations, expression of constitutively active AR variants, and intracrine steroid synthesis, as well as AR bypass mechanisms [1]. It has been shown that several new drugs prolong survival and increase quality of life for men with CRPC, including novel AR antagonists, cytostatic drugs, radioisotopes, steroidogenesis inhibitors, immunotherapies, and therapies targeting the tumor microenvironment [2]. Thus, there is a need for biomarkers that can guide CRPC therapy selection. Moreover, the fatal outcome for patients with CRPC highlights the necessity for further therapeutic developments, particularly for patients characterized by low AR activity and for whom no targeting therapy currently exists.

We previously identified heterogeneous gene expression patterns of clinical relevance in metastatic CRPC samples, and found that high levels of the constitutively active AR variant 7 (AR-V7) were associated with particularly poor prognosis [3]. Antonarakis and co-workers showed that detectable levels of AR-V7 in circulating tumors cells are predictive of poor response to AR-targeted therapies [4]. We also found a heterogeneous expression pattern for the steroidogenic enzyme AKR1C3 in clinical samples of CRPC metastases [5], and the relevance of AKR1C3 as a predictive marker for therapy response to the steroidogenesis inhibitor abiraterone is currently under evaluation.

The aim of this study was to further characterize gene expression in bone metastases from men with CRPC to identify subgroups of relevance for therapy choice.

2. Patients and methods

2.1. Patients

Fresh-frozen bone metastasis samples were obtained from a series of men with PC ($n = 65$) or other malignancies ($n = 14$) who underwent surgery for metastatic spinal cord compression at Umeå University Hospital between 2003 and 2013. The PC patient series has been described before [3,5,6] and the clinical characteristics are summarized in Table 1. Formalin-fixed, paraffin-embedded (FFPE) metastasis samples were available for 41 of the 54 CRPC patients in Table 1 and matched diagnostic prostate biopsies were available in 29 cases, obtained at a median of 37 mo (interquartile range [IQR] 16–79) before the metastasis biopsy. The study also included 12 separate men who were treated with radical prostatectomy at Umeå University Hospital between 2005 and 2006; the median age for these men was 61 yr (IQR 57–67) and median prostate-specific antigen (PSA) was 11 ng/ml (IQR 5.3–18 ng/ml). Clinical local stage was T2 ($n = 3$) or T3 ($n = 9$) and Gleason score (GS) was 7 ($n = 10$) or 8 ($n = 2$).

Tissue microarrays (TMAs) were previously constructed from samples taken during transurethral resection of the prostate (TURP) performed between 1975 and 1991 as previously described [7]. Gleason score was reevaluated by one pathologist (L.E.) and TMAs were constructed containing five to eight samples of tumor tissue and four samples of nonmalignant tissue from each patient. For this study, TMAs from 284 patients had tissue available for analysis (Supplementary Table 1). The patients had not received cancer therapy before TURP and, according to the therapy traditions in Sweden at that time, the majority ($n = 202$) were managed via watchful waiting.

The study was approved by the local ethics review board of Umeå University (Dnr 03-185, 2010-240-32, and 02-283).

2.2. Tissue preparation

Bone metastasis samples were instantly fresh-frozen in liquid nitrogen or placed in 4% buffered formalin. Fixed samples were decalcified in formic acid before being embedded in paraffin. Fresh radical prostatectomy specimens were received at the pathology department immediately after surgery and cut in 0.5-cm-thick slices before fixation. From these slices, 20 samples were taken using a 0.5-cm skin punch and frozen in liquid nitrogen within 30 min after surgery. The prostate slices were formalin-fixed, embedded in paraffin, cut in 5 μm-thick sections, whole-mounted, and stained with hematoxylin-eosin. Tissue sample composition (nonmalignant or malignant) was determined according to location in the whole-mount sections.

2.3. RNA extraction

Representative areas of fresh-frozen bone metastasis samples and of malignant and nonmalignant prostate tissue (obtained in pairs from the same patient) were cryosectioned into extraction tubes and RNA was isolated using the Trizol (Invitrogen, Stockholm, Sweden) or AllPrep (Qiagen, Stockholm, Sweden) protocol. The percentage of tumor cells in the samples was determined by examination of parallel sections stained with hematoxylin-eosin, and varied between 50% and 90%. The RNA concentrations were quantified by absorbance measurements using a spectrophotometer (ND-1000; NanoDrop Technologies, Wilmington, DE, USA). The RNA quality was analyzed on a 2100 Bioanalyzer (Agilent Technologies, Santa Clara, CA, USA) and verified to have a RNA integrity number $\geq$6.

2.4. Whole-genome expression profiling

For each sample, 300 ng of total RNA was amplified using an Illumina TotalPrep RNA amplification kit (Ambion, Austin, TX, USA) according to the manufacturer's protocol. A total of 750 ng of cRNA from each sample was hybridized to HumanHT-12 v4 Expression BeadChips, including more than 47 000 probes covering over 31 000 annotated genes,

Please cite this article in press as: Ylitalo EB, et al. Subgroups of Castration-resistant Prostate Cancer Bone Metastases Defined Through an Inverse Relationship Between Androgen Receptor Activity and Immune Response. Eur Urol (2016), http://dx.doi.org/10.1016/j.eururo.2016.07.033

Table 1 – Clinical characteristics for patients with prostate cancer or other malignancies who underwent surgery for metastatic spinal cord compression

	Prostate cancer		Other malignancies [b]
	Castration-resistant [a]	Not treated	Not treated
Patients (*n*)	54	11	14
Age at diagnosis (yr)	69 (63-74)	76 (64-82)	67 (61-79)
Age at metastasis surgery (yr)	72 (67-79)	76 (64-82)	67 (61-79)
Serum PSA at diagnosis (ng/ml)	72 (36-530)	690 (82-2500)	–
Serum PSA at metastasis surgery (ng/ml)	290 (85-780)	690 (82-2500)	–
Gleason score at diagnosis			–
6	4 (7.4)	1 (9.1)	
7	19 (35)	1 (9.1)	
8–10	20 (37)	1 (9.1)	
Not available	11 (20)	8 (73)	
Bicalutamide before surgery		–	–
Yes	24 (44)		
No	30 (56)		
Chemotherapy before surgery [c]		–	–
Yes	9 (17)		
No	45 (83)		
Radiation before surgery [d]		–	–
Yes	8 (15)		
No	46 (85)		
Follow-up after metastasis surgery (mo)	5.9 (2.0-15)	37 (24-72)	7.0 (3.6-16)

Data are presented as median (25th–75th percentile) for continuous variables and as number (precentage) for categorical variables. PSA = prostate-specific antigen.
[a] Castration-resistant patients had disease progression after long-term androgen deprivation therapy including surgical ablation, luteinizing hormone–releasing hormone/GNRH agonist therapy, and therapy with anti-androgens (bicalutamide).
[b] Other malignancies included kidney (*n* = 3), colorectal (*n* = 2), lung (*n* = 1), liver (*n* = 1), unknown adenocarcinoma (*n* = 3), myeloma (*n* = 2), lymphoma (*n* = 1), and sarcoma (*n* = 1).
[c] Chemotherapy included taxotere in six cases, estramustine in two cases, and taxotere, carboplatin, and etoposide in one case.
[d] Radiation towards operation site.

according to the manufacturer's protocol. Beadchips were scanned using a HiScan system (Illumina, San Diego, CA, USA) and analysis of array data was performed using GenomeStudio software (version 2011.1, Illumina). Samples were normalized by the cubic spline algorithm, and probes with all signals lower than two times the mean background level were excluded, leaving 21 675 probes for further analysis.

2.5. Multivariate modeling and univariate analysis

Principal component analysis (PCA), an unsupervised projection method, was used to create an overview of the variation in data and to detect clusters and trends among metastasis samples and expressed genes [8]. Data were mean-centered and scaled to unit variance before analysis. Models were validated via sevenfold cross-validation. Multivariate statistical analyses were performed in SIMCA version 14.0 (MKS Umetrics AB, Umeå, Sweden).

Univariate analysis was applied to compare subgroups identified by PCA with respect to differences in gene expression and clinical characteristics. Groups were compared using the Mann-Whitney *U*-test for continuous variables and the χ^2 for categorical variables. Univariate statistical analyses were performed using SPSS 23.0 software (SPSS, Chicago, IL, USA).

2.6. Functional enrichment analysis

Functional enrichment analysis was generated via Ingenuity Pathway Analysis (IPA; www.qiagen.com/ingenuity). IPA core analysis was used to identify altered canonical pathways. The significance of associations between lists of differently expressed genes and canonical pathways were assessed using (1) the ratio of differentially expressed genes (molecules) that map to a specific pathway, given in relation to the total number of molecules included in the canonical pathway and (2) Fisher's exact test to determine the probability that the relationship between the molecules in the data set and the canonical pathway is explained by chance.

Upstream analysis was used to identify regulators with a probability of being responsible for the changes in gene expression observed, by calculating an overlap *p* value with Fisher's exact test and an activation *z*-score. Details of the IPA core analysis can be obtained at http://pages.ingenuity.com/IngenuityDownstreamEffectsAnalysisinIPAWhitepaper.html. Both upregulated and downregulated identifiers were submitted as parameters for the analysis. IPA core analysis default settings were used, but limited to the human knowledge base.

2.7. Real-time RT-PCR

Samples of 200 ng of total RNA were reversed transcribed using a Superscript VILO cDNA synthesis kit (Invitrogen, Stockholm, Sweden) in a total volume of 10 μl. Subsequent qRT-PCR analysis was performed using TaqMan assays for quantification of *HLA-A*, *TAP1*, and *PSMB9* mRNA levels (Hs01058806_g1, Hs00388675_m1, and Hs00160610_m1; Life Technologies, Stockholm, Sweden) on an ABI Prism 7900HT sequence detection system according to the manufacturers' protocols. Each sample was run in duplicate and adjusted for the corresponding *RPL13A* mRNA level (Hs01578912_m1, Life Technologies) using the ddCt method. Statistical differences in mRNA levels between groups were identified using the Kruskal-Wallis test followed by the Mann-Whitney *U*-test. Paired samples were compared using the Wilcoxon signed-rank test.

2.8. Immunohistochemistry

Tissue sections were deparaffinized in xylene and rehydrated in a graded ethanol series. Immunohistochemistry was performed using an

Please cite this article in press as: Ylitalo EB, et al. Subgroups of Castration-resistant Prostate Cancer Bone Metastases Defined Through an Inverse Relationship Between Androgen Receptor Activity and Immune Response. Eur Urol (2016), http://dx.doi.org/10.1016/j.eururo.2016.07.033

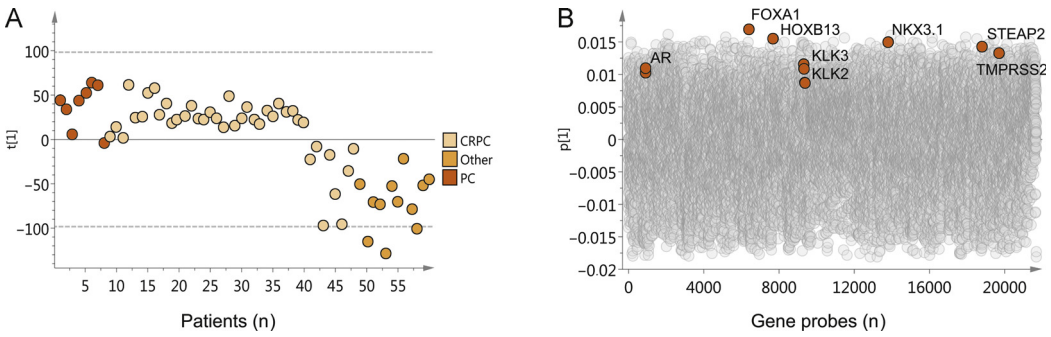

Fig. 1 – Principal component analysis of 2 1675 assigned gene products in 60 bone metastases samples. (A) Score plot for the first principal component. Each dot corresponds to one metastasis sample collected from untreated prostate cancer (PC) patients (orange), castration-resistant prostate cancer (CRPC) patients (beige), and patients with other malignancies (yellow). Samples cluster according to their relative gene expression. (B) Loading plot showing gene probes responsible for the clustering of samples. Gene probes with positive loading values (p) are expressed at high levels in samples with positive score values (t) and vice versa. Black circles denote the gene probes for AR, FOXA1, HOXB13, KLK3, KLK2, NKX3.1, STEAP2, and TMPRSS2.

ultraView Universal DAB detection kit with the CC1 antigen retrieval technique on an automatic Ventana Benchmark Ultra system according to the manufacturer's protocol (Roche Diagnostics, Basel, Switzerland), with primary antibodies for CD3 (1:50, NCL-L-CD3-565; Novocastra, Newcastle upon Tyne, UK), CD68 (1:2000, M0814; Dako, Glostrup, Denmark), HLA class I ABC (1:200, ab70328; Abcam, Cambridge, UK), and FOXA1 (1:200, ab23738; Abcam). The AR was detected after antigen retrieval in Tris/EDTA (pH 9) with anti-AR (1:150, MUC256-UCE; Biogenex, Fremont, CA, USA) and an IPflx system (Biocare Medical, Concord, CA, USA) using a Mach3 mouse kit with DAB as chromogen. For double staining, HLA ABC was detected with Ap RED as chromogen following AR detection after incubation of sections for 5 min in denaturation buffer (DNS001H; Biocare Medical). The volume density of $CD68^+$ cells was determined using a square lattice mounted in the eyepiece of a light microscope and counting cross-sections falling on stained cells or reference tissue, and expressed as the average density per tissue after evaluation of at least ten randomly selected fields. Metastasis-infiltrating $CD3^+$ cells were less abundant than $CD68^+$ cells and were therefore evaluated as the number of positive cells in the total stained tumor area using a Pannoramic 250 FLASH scanner and Pannoramic viewer 1.15.2 software (3DHISTECH, Budapest, Hungary). HLA class I ABC staining intensity was scored as negative (0), weak (1), moderate (2), or intense (3), and the most common score per sample/TMA core was recorded. For survival analysis, each patient was represented by the less stained TMA core (median and maximum intensities were evaluated, with similar results; data not shown). Nuclear AR immunoreactivity in tumor cells was scored according to intensity (0 = negative, 1 = weak, 2 = moderate, 3 = intense staining) and fraction of cells stained (1 = 1–25%, 2 = 26–50%, 3 = 51–75%, 4 = 76–100%). A total score (ranging from 0 to 12) was obtained by multiplying the staining intensity and fraction scores, as previously described [6]. When comparing immunoreactivity between two groups, the Mann-Whitney *U*-test and χ^2 test were used for continuous and categorical variables, respectively. Survival analysis was performed using the Kaplan-Meier method, with death from PC as events and death from other causes as censored events. Correlations between variables were analyzed using the Spearman rank test.

3. Results

3.1. Whole-genome expression analysis identifies CRPC subgroups according to AR activity

A set of fresh-frozen bone metastases from CRPC patients (n = 40) was characterized and compared to bone metastases from eight untreated PC patients and 12 untreated male patients with other primary malignancies using whole-genome expression profiling and multivariate PCA. The PCA model resulting from analysis of 21 675 gene probe signals included nine significant principal components explaining 45% of the total variation in the expression data. The first component describing the largest variation in the data (R2X=11%, Q2=7%), and thus the most prominent subgroups, was selected for further investigation. It is evident in Figure 1A that the majority of the CRPC bone metastasis samples cluster close to the untreated PC metastases, while some CRPC samples cluster closer to metastases of other malignancies. According to the score values for the first principal component **t**1 in Figure 1A, the CRPC samples were divided into two groups; samples with positive scores showing high transcript levels of the AR, the AR co-regulators FOXA1 and HOXB13, and androgen-regulated genes such as *KLK2*, *KLK3*, *NKX3.1*, *STEAP2*, and *TMPRSS2*; and samples with negative scores showing low levels of these gene transcripts (Fig. 1B). Univariate analysis of differentially expressed genes identified the AR and many AR-regulating and/or AR-regulated gene transcripts among the top genes with positive fold changes in samples with positive compared to negative PCA scores (Supplementary Table 2). On the basis of these findings, the 32 CRPC samples with positive PCA scores (80%) were defined as AR-driven and the eight CRPC samples with negative PCA scores (20%) as non–AR-driven. Notably, patients with AR-driven CRPC metastases had higher serum PSA levels than patients with non–AR-driven metastases at the time of metastasis surgery (and borderline higher PSA at diagnosis). No obvious association with previous treatments, presence of soft tissue metastasis, or cancer-specific survival after metastasis surgery was found (Supplementary Table 3).

3.2. Functional differences between AR-driven and non–AR-driven CRPC bone metastases

To examine functional differences between AR-driven and non–AR-driven CRPC samples, the list of differently expressed genes (fold change $\geq \pm$ 1.5 and p P$\leq$0.01, Supplementary Table 2) was imported into the Qiagen

Ingenuity Pathway Analysis tool for assignment of altered canonical pathways and identification of upstream regulators. According to analysis of 617 upregulated and 906 downregulated gene transcripts, AR-driven CRPC metastases had higher metabolic activity for biosynthesis of cholesterol, pyrimidines, and spermine and degradation of fatty acids and amino acids when compared to non–AR-driven samples (Table 2). Among the downregulated canonical pathways in AR-driven metastases, the cellular immune response was the most obvious (Table 2). Upstream regulators predicted as responsible for the differential expression observed between AR-driven and non–AR-driven CRPC bone metastases are listed in Supplementary Table 4. *AR*, *SPDEF*, and *FOXA1* were among the top activated genes that also showed increased mRNA levels in AR-driven metastases, while several immune regulating genes such as *TGFB1*, *INFG*, and other cytokines were predicted to be inhibited, and some (*CCL5*, *ETV5*, *PLAUR*, and *IFNAR2*) also showed reduced mRNA levels (Supplementary Table 4).

The predicted difference in cellular immune response was verified by immunohistochemical analysis of $CD3^+$ and $CD68^+$ cells in CRPC bone metastases in FFPE tissue available, which revealed a significantly higher volume density of $CD68^+$ monocytes and borderline higher frequency of $CD3^+$ infiltrating lymphocytes in non–AR-driven compared to AR-driven bone metastases (Figure 2A–D). Gene expression data indicated higher levels of $CD3^+$ T cells, and specifically of $CD8^+$ effector T cells and $CD4^+$ helper T cells in non–AR-driven compared to AR-driven metastases (Supplementary Fig. 1A–C). This was accompanied by increased levels of the inhibitory T cell receptors CTLA4 and PDCD1 and lower levels of the proinflammatory Th1 transcription factor TBX21 (Supplementary Fig. 1D–F), while levels of the stimulatory T-cell receptors ICOS and CD28 and the anti-inflammatory Th2 transcription factor GATA did not differ between non–AR-driven and AR-driven metastases (data not shown). We did not detect mRNA for the regulatory T cell (Treg) transcription factor FOXP3. Non–AR-driven cases had higher levels of *CD68*, *CD163*, and *S100A9* mRNA (Supplementary Fig. 1G–I) but not *NOS2* mRNA (data not shown), indicating metastasis infiltration of tumor-promoting M2 macrophages and myeloid-derived suppressor cells (MDSCs).

The downregulated antigen presentation observed in AR-driven CRPC bone metastases (Table 2 and Supplementary Fig. 2) possibly contributed to the low immune-cell infiltration, and this pathway was therefore selected for further examination.

3.3. Downregulation of MHC class I expression during PC progression

To verify the PCA findings, we analyzed the expression levels of genes involved in MHC class I antigen processing

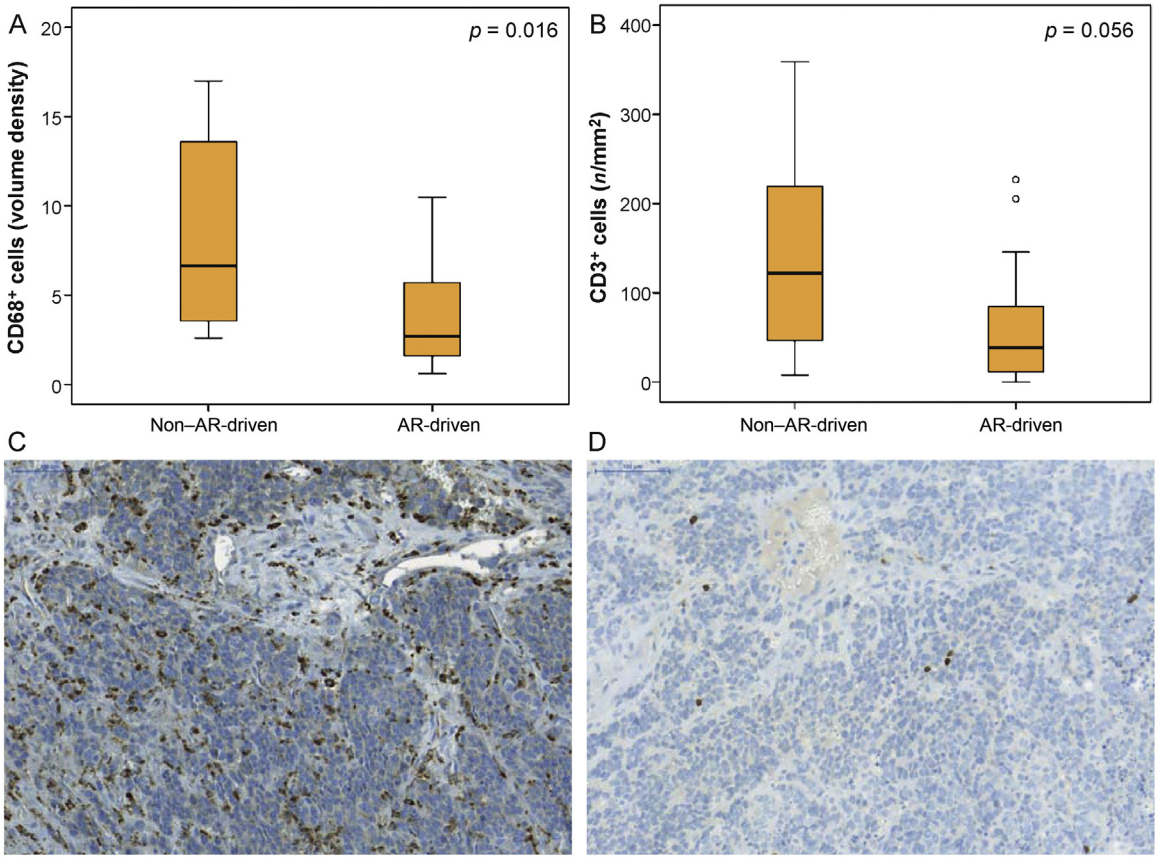

Fig. 2 – Immunohistochemical analysis demonstrating (A) significantly higher infiltration of $CD68^+$ immune cells and (B) borderline higher infiltration of $CD3^+$ immune cells in non–AR-driven ($n = 8$) compared to AR-driven ($n = 26$) castration-resistant prostate cancer bone metastases. Sections show representative (C) CD68 and (D) CD3 staining of a non–AR-driven metastasis sample.

Table 2 – Canonical pathways predicted by Ingenuity pathway analysis to be upregulated or downmodulated in AR-driven compared to non-AR-driven castration-resistant prostate cancer bone metastases according to whole-genome array analysis and principal component analysis

Ingenuity canonical pathway	*p* value [a]	Ratio	Category	Molecules
Upregulated				
Cholesterol biosynthesis superpathway	0.004	0.26	Sterol biosynthesis	DHCR7, ACAT2, MSMO1, HMGCS2, HMGCR, TM7SF2, SC5D
Methionine degradation superpathway	0.005	0.23	Methionine degradation	CBS/CBSL, DLD, PCCB, CTH, MUT, SUOX, AHCY
Fatty acid β-oxidation I	0.025	0.20	Fatty acid degradation	ACSL3, SLC27A2, ECI2, AUH, IVD, HSD17B4
2-Oxobutanoate degradation I	0.025	0.60	2-Oxobutanoate degradation	DLD, PCCB, MUT
Cholesterol biosynthesis	0.025	0.31	Sterol biosynthesis	DHCR7, MSMO1, TM7SF2, SC5D
Pyrimidine ribonucleotide interconversion	0.032	0.19	Pyrimidine nucleotide biosynthesis	NME3, NME4, ENTPD6, AK4, CANT1
β-Alanine degradation I	0.032	1.0	B-Alanine degradation	ABAT, ALDH6A1
Spermine biosynthesis	0.032	1.0	Amine and polyamine biosynthesis	SMS, AMD1
Cysteine biosynthesis/ homocysteine degradation	0.032	1.0	Homocysteine degradation, cysteine biosynthesis	CBS/CBSL, CTH
Pyrimidine ribonucleotide de novo biosynthesis	0.042	0.18	Pyrimidine nucleotide de novo biosynthesis	NME3, NME4, ENTPD6, AK4, CANT1
Downregulated				
Hepatic fibrosis / hepatic stellate cell activation	2e-08	0.18	Disease-specific pathways; ingenuity toxicity list pathways	IGFBP4, FN1, MYH9, SMAD3, KLF6, COL8A1, CCL5, PDGFC, COL15A1, COL5A1, IL1R2, COL1A2, TIMP1, PDGFRA, COL22A1, COL18A1, KLF12, TNFRSF1B, TIMP2, PDGFRB, TNFRSF11B, VCAM1, COL5A2, MMP2, IFNAR2, COL1A1, TLR4, LY96, COL6A3, CD40, IL10RA, CD14
Antigen presentation pathway	7e-08	0.38	Cellular immune response; humoral immune response	HLA-G, B2M, PSMB9, HLA-DRB4, HLA-DRB1, HLA-DMA, HLA-A, HLA-B, CD74, PSMB8, HLA-F, TAPBP, HLA-E, MR1
Leukocyte extravasation signaling	1e-07	0.16	Cellular immune response	RAC2, CLDN11, MMP16, TIMP1, CYBA, CYBB, RASSF5, ACTN1, ACTA1, TIMP2, VCAM1, CXCR4, ACTB, ARHGAP4, ITGA5, THY1, MMP2, NCF4, GNAI2, BTK, ITGB2, WIPF1, ITGAM, ARHGAP9, WAS, JAM3, PLCG2, PIK3CD, ACTN4, PRKCB, MSN
Caveolar-mediated Endocytosis Signaling	1E-06	0.24	Cellular Immune Response; Organismal Growth and Development; Pathogen-Influenced Signaling	B2M, FYN, HLA-A, ACTB, HLA-B, CD48, ITGA5, ITGB7, ITGB2, ITGAM, FLNC, ITGA11, ITGA9, CAV1, ITGB4, ACTA1, ITGAX
Crosstalk between Dendritic Cells and Natural Killer Cells	1E-06	0.21	Cellular Immune Response	TYROBP, HLA-A, ACTB, CD69, HLA-B, LTB, HLA-G, TLR4, PRF1, HLA-DRB1, HLA-DRB4, MICB, CD40, FSCN1, CD86, TNFRSF1B, HLA-F, ACTA1, HLA-E
Allograft rejection signaling	1e-06	0.29	Cellular immune response; disease-specific pathways	HLA-G, B2M, PRF1, HLA-DRB4, HLA-DRB1, CD40, HLA-DMA, GZMB, HLA-A, HLA-B, FCER1G, CD86, HLA-F, HLA-E
Complement system	2e-06	0.33	Humoral immune response	C1R, ITGB2, CFD, ITGAM, C5AR1, CFB, CFI, C1QC, C1QA, C1QB, C2, ITGAX
Dendritic cell maturation	3e-06	0.15	Cellular immune response; cytokine signaling; pathogen-influenced signaling	B2M, PLCB2, TYROBP, FCGR2A, HLA-A, HLA-B, LTB, PLCL2, FCGR1A, COL1A2, COL1A1, TLR4, HLA-DRB4, HLA-DRB1, CD40, HLA-DMA, DDR2, FSCN1, PLCG2, FCER1G, CD86, PIK3CD, IRF8, COL18A1, TNFRSF1B, TNFRSF11B
Integrin signaling	6e-06	0.14	Cell cycle regulation; cellular growth, proliferation and development; intracellular and second messenger signaling	RAC2, RAP2A, FYN, MPRIP, TSPAN7, ARPC5, ITGB7, RHOG, ITGA11, ITGA9, CAV1, ITGB4, TSPAN4, ACTA1, ACTN1, ASAP1, ACTB, ITGA5, RHOJ, GSN, ITGB2, WIPF1, ITGAM, WAS, PLCG2, PIK3CD, ACTN4, ITGAX
Phagosome formation	7E-06	0.19	Cellular Immune Response; Pathogen-Influenced Signaling	PLCB2, FN1, MRC2, FCGR2A, TLR8, ITGA5, RHOJ, PLCL2, FCGR1A, INPP5D, TLR4, RHOG, SCARA3, PLCG2, SYK, FCER1G, PIK3CD, MARCO, PRKCB

[a] P value after FDR correction according to Benjamini-Hochberg.

and presentation (*PSMB9*, *TAP1*, and *HLA-A*) in an extended set of CRPC bone metastasis samples ($n = 53$), non-treated PC metastases ($n = 11$), and non-treated metastases from other malignancies ($n = 13$; Fig. 3). Levels in metastases were compared to levels in paired samples of non-malignant and malignant prostate tissue from radical prostatectomies ($n = 12$). *PSMB9*, *TAP1*, and *HLA-A* mRNA levels in bone metastases were significantly lower in PC patients than in patients with other malignancies (Fig. 3A–C). However, and in accordance with the array data, the CRPC bone metastases could be classified into two groups on the basis of their variation in *PSMB9*, *TAP1*, and *HLA-A* mRNA levels (Fig. 3D), suggesting MHC class I antigen presentation was downregulated in the majority of CRPC

Please cite this article in press as: Ylitalo EB, et al. Subgroups of Castration-resistant Prostate Cancer Bone Metastases Defined Through an Inverse Relationship Between Androgen Receptor Activity and Immune Response. Eur Urol (2016), http://dx.doi.org/10.1016/j.eururo.2016.07.033

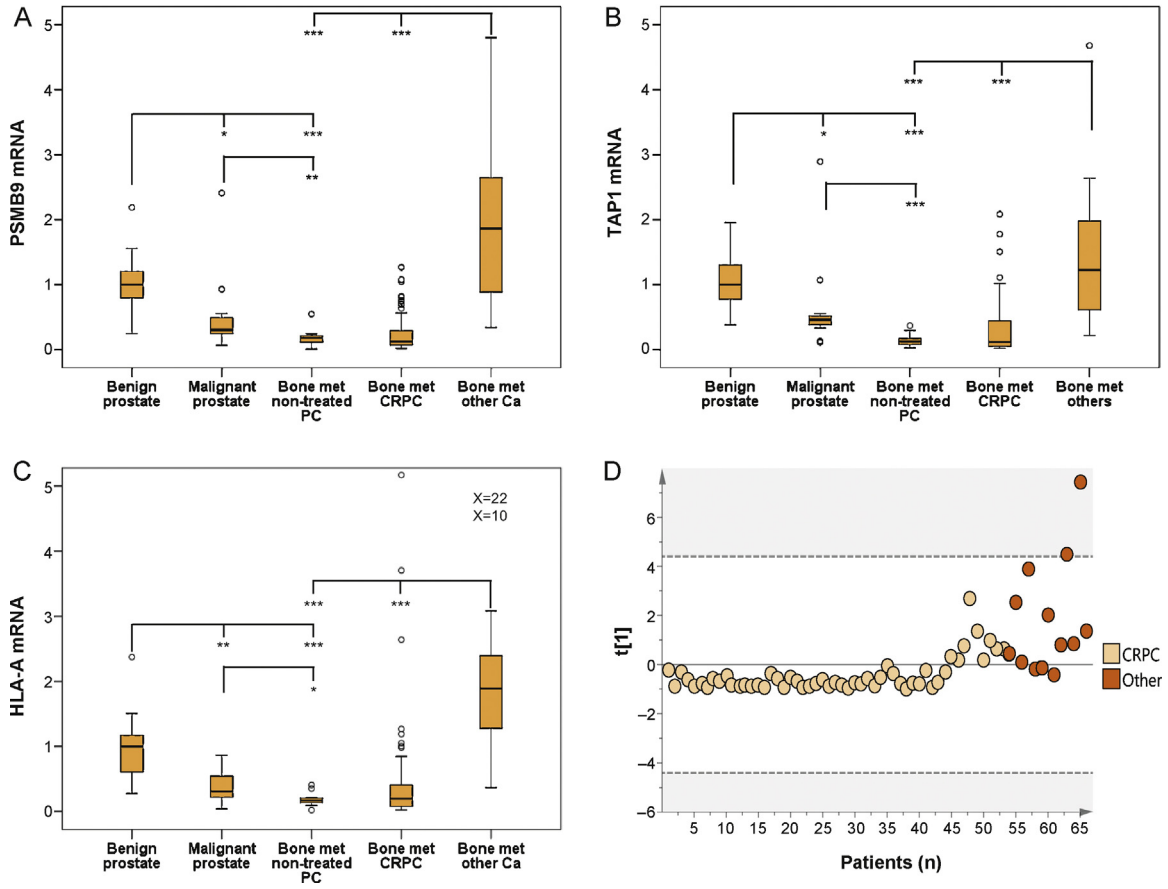

Fig. 3 – Relative mRNA levels of (A) *PSMB9*, (B) *TAP1*, and (C) *HLA-A* in paired nonmalignant and malignant prostate tissue samples from patients treated with radical prostatectomy ($n = 12$) and in non-treated ($n = 11$) and castration-resistant prostate cancer (CRPC) bone metastases ($n = 53$) and bone metastases from other malignancies ($n = 13$). * $p < 0.05$, ** $p < 0.01$, *** $p < 0.001$. (D) Principal component analysis of bone metastases samples from CRPC patients (beige) and patients with other malignancies (orange). Score plot for the first principal component, for which each dot corresponds to one patient sample. Samples cluster according to their relative *PSMB9*, *TAP1*, and *HLA-A* mRNA levels. met = metastases.

bone metastases but preserved in a subgroup of cases. Notably, *PSMB9*, *TAP1*, and *HLA-A* mRNA levels were all significantly lower in malignant compared to nonmalignant prostate tissue and were even lower in bone metastasis tissue (Fig. 3A–C).

Accordingly, immunoreactivity for HLA class I ABC was lower in metastases than in matched primary tumor biopsies obtained at diagnosis (median 37 mo [IQR 16–79 mo] before metastasis surgery; $p = 0.037$, $n = 29$; data not shown), indicating a reduction in MHC class I protein expression during PC disease progression.

3.4. Inverse correlation between MHC class I expression and nuclear AR immunoreactivity in CRPC metastases

The PCA model indicated downregulated MHC class I antigen presentation in AR-driven CRPC bone metastases compared to preservation of MHC class I antigen presentation in non–AR-driven CRPC bone metastases, so we studied HLA class I ABC immunoreactivity in relation to nuclear AR immunoreactivity (previously measured in those metastases and assumed to reflect AR activity [6]). HLA class I ABC immunoreactivity in tumor cells was evaluated in metastases for which FFPE tissue was available, and was found to be inversely correlated to the nuclear AR score (Rs = −0.49, $p = 0.001$, $n = 41$; Fig. 4 A–D). Importantly, metastases with moderate to intense HLA class I ABC immunoreactivity showed a significantly higher frequency of $CD3^+$ infiltrating cells than cases with negative to weak immunostaining (Supplementary Fig. 3).

Staining heterogeneity was observed for both AR and HLA class I ABC immunoreactivity in many cases, so double staining was performed. Nuclear AR showed a clear inverse staining pattern to HLA class I ABC (Fig. 4E). FOXA1 staining in consecutive sections indicated reduced but not completely diminished FOXA1 levels in AR-negative/HLA class I ABC–positive tumor cells (Fig. 4F).

3.5. Reduced expression of HLA class I ABC in primary prostate tumors with advanced disease stage

To evaluate if MHC class I expression in primary PC is related to patient prognosis, HLA class I ABC immunoreactivity was evaluated in a TMA including transurethral cancer biopsies from 284 patients with long clinical follow-up and in adjacent benign tissue in 179 cases. Malignant epithelial cells showed less intense staining than adjacent benign epithelial cells ($p < 0.0001$; Fig. 5A). Lower HLA ABC

Please cite this article in press as: Ylitalo EB, et al. Subgroups of Castration-resistant Prostate Cancer Bone Metastases Defined Through an Inverse Relationship Between Androgen Receptor Activity and Immune Response. Eur Urol (2016), http://dx.doi.org/10.1016/j.eururo.2016.07.033

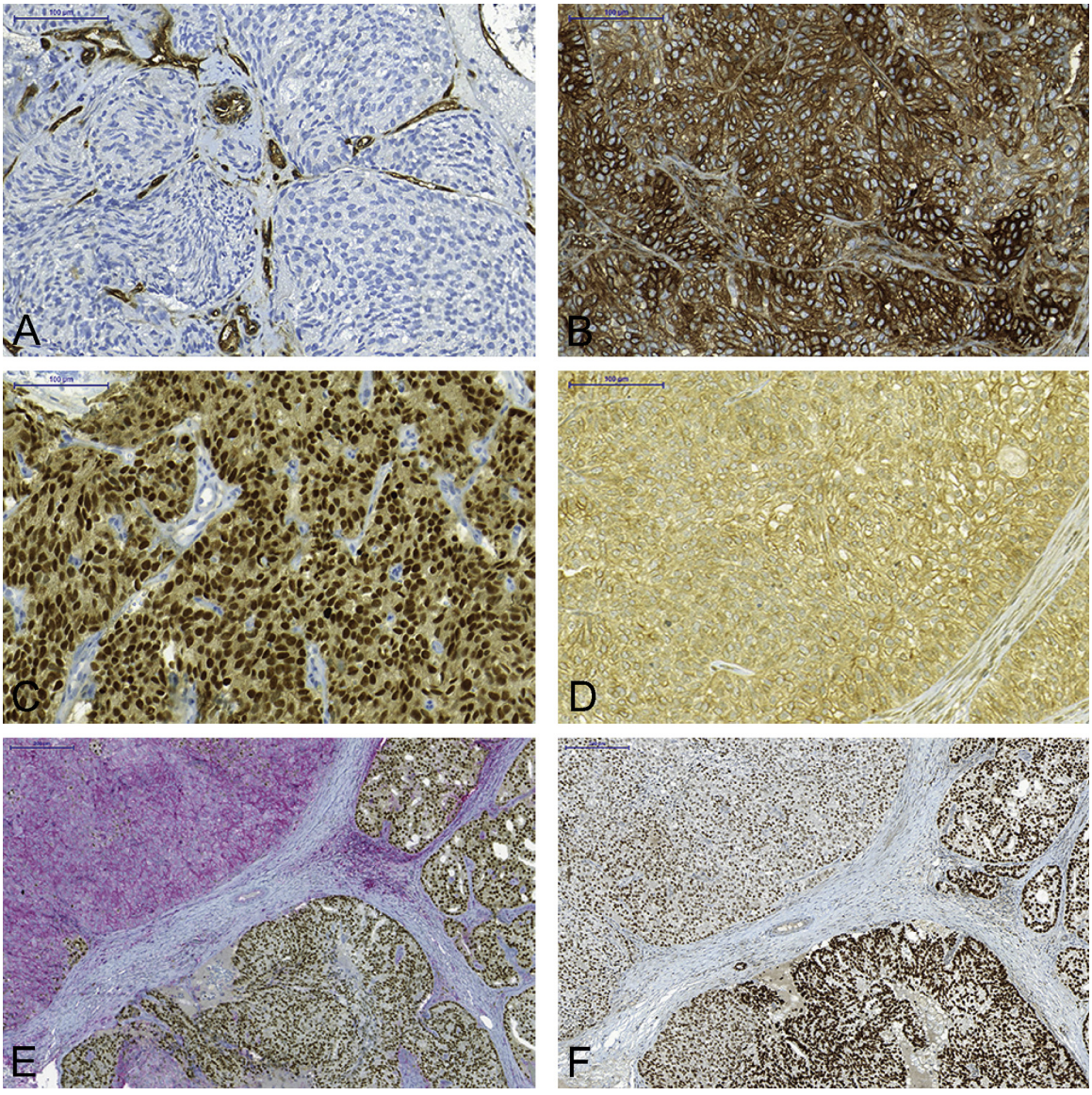

Fig. 4 – Immunohistochemistry for (A,B) HLA class I ABC and (C,D) androgen receptor (AR) in bone metastasis tissue sections from patients with castration-resistant prostate cancer (CRPC). One patient exhibits negative HLA class I staining (A) and intense nuclear AR staining (C) while the other exhibits intense HLA class I staining (B) and negative nuclear AR staining. (E) Double staining for HLA class I ABC (red) and AR (brown) in CRPC metastasis and (F) immunohistochemistry for FOXA1 in a parallel metastasis section. Magnification according to scale bars in the figure.

staining of tumor cells was associated with higher GS and the presence of metastases at diagnosis (Supplementary Table 1). In addition, when patients with metastases (M1) at diagnosis were excluded from the analysis, patients with low (negative to weak) HLA ABC immunoreactivity had shorter cancer-specific survival than patients with moderate to intense immunoreactivity (Fig. 5B; $p = 0.047$, $n = 248$). In patients managed with watchful waiting ($n = 202$), a similar but nonsignificant trend was seen (Fig. 5C; $p = 0.13$).

4. Discussion

We found two subgroups among CRPC bone metastases, defined by high AR activity and low cellular immune responses, or low AR activity and high cellular immune responses. Moreover, CRPC bone metastases with high AR activity seemed to have higher metabolic activities than metastases with low AR activity. To the best of our knowledge, these two CRPC subgroups have not previously been described. Our results confirm previous findings of lower levels of PSMB9, TAP1, and HLA class 1 molecules in PC compared to benign prostate tissue [9–11]. Importantly, we also present novel data indicating an association between low tumor HLA class I ABC immunoreactivity at diagnosis and poor clinical outcome, as well as markedly lower HLA class I expression in PC bone metastases compared to primary tumors.

The subgroups observed had similar expression levels of neuroendocrine and cancer stem-cell markers (Supplementary Table 2), and we found no enrichment of tumors negative for MHC class I among docetaxel-treated

Please cite this article in press as: Ylitalo EB, et al. Subgroups of Castration-resistant Prostate Cancer Bone Metastases Defined Through an Inverse Relationship Between Androgen Receptor Activity and Immune Response. Eur Urol (2016), http://dx.doi.org/10.1016/j.eururo.2016.07.033

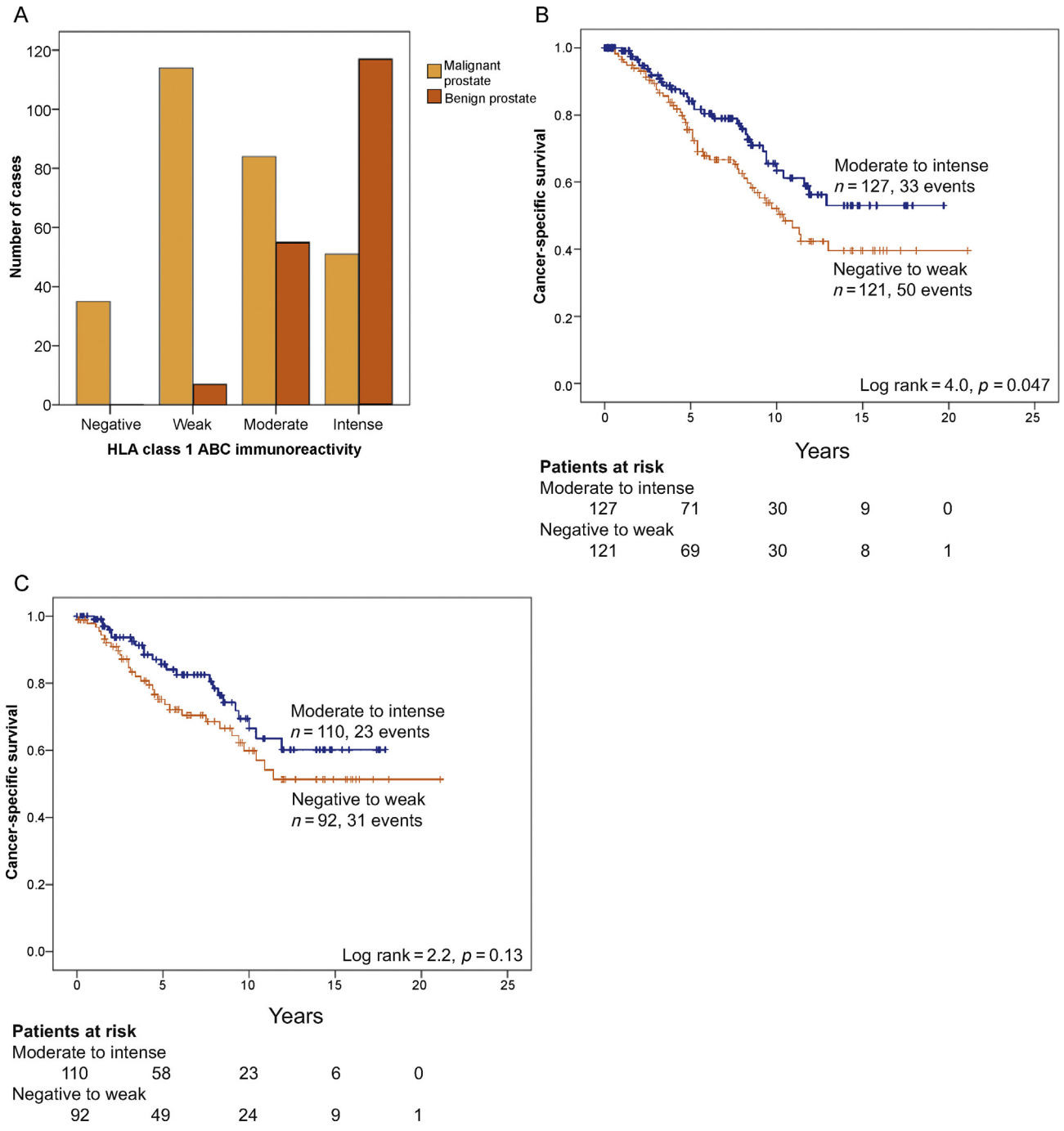

Fig. 5 – Tumor immunoreactivity for HLA class I ABC in a historical cohort of patients diagnosed via transurethral section of the prostate showing (A) reduced staining intensity in malignant ($n = 284$) compared to adjacent nonmalignant ($n = 179$) epithelium ($p < 0.001$) and shorter cancer-specific survival in patients with lower HLA class I tumor cell immunoreactivity (negative to weak) compared to patients with moderate to intense immunoreactivity in (B) patients without metastases at diagnosis ($p = 0.047$, $n = 248$), and (C) patients treated with watchful waiting ($p = 0.13$, $n = 202$).

patients, as previously reported [12]. Not surprisingly, however, *AR-V7* mRNA levels were much higher in the AR-driven than in non–AR-driven CRPC metastases, while no differences in *AKR1C3* mRNA levels were seen (data not shown and Supplementary Table 2). In addition to AR-targeted therapies, we hypothesize that patients with AR-driven CRPC metastases might benefit from therapies targeting cholesterol biosynthesis, β-oxidation, and polyamine synthesis, pathways that were particularly upregulated in this subgroup. This is in line with previous findings by our group of high cholesterol levels and β-oxidation in CRPC bone metastases [13,14]. Furthermore, we hypothesize that patients with non–AR-driven CRPC metastases with preserved MHC class I expression will be resistant to all forms of anti-AR therapy, but might instead be susceptible to cancer immunotherapy.

Please cite this article in press as: Ylitalo EB, et al. Subgroups of Castration-resistant Prostate Cancer Bone Metastases Defined Through an Inverse Relationship Between Androgen Receptor Activity and Immune Response. Eur Urol (2016), http://dx.doi.org/10.1016/j.eururo.2016.07.033

Cancer immunotherapy is based on the fact that cancer cells are immunogenic, and the aim of immunotherapy is to strengthen the endogenous antitumor response via immunologic interventions [15]. Tumors develop in an immune-suppressed environment in which cytotoxic $CD8^+$ T cells and NK cells are repressed by inhibitory factors expressed by tumor cells, Tregs, and MDSCs, and in which MDSCs and type M2 macrophages instead promote tumor growth via secretion of factors that stimulate angiogenesis and tumor cell invasion [15,16]. Most cancer immunotherapies are developed to strengthen cytotoxic T and NK cell activity via tumor vaccination or to inhibit immune checkpoint pathways such as the CTLA-4 or PDCD1/PD-L1 pathways [15].

Very little is known about the immune cell profile in PC metastases. In primary PC, low tumor infiltration of T cells, B cells, and monocytes has been observed in advanced disease and associated with poor prognosis [17], although recent studies highlight tumor infiltration of specific lymphocyte/monocyte subtypes, such as $FoxP3^+$ Tregs, $CD163^+$ M2 macrophages, and S100A9-positive inflammatory cells, in lethal PC [18–22]. High blood fractions of Tregs and MDSC have been related to poor prognosis in patients with CRPC [23], as have a whole-blood–based mRNA profile mirroring high monocyte/low lymphocyte numbers [24]. Overall, this points to the rationale for using immunotherapy for treatment of PC. Immunotherapies that are being tested in the clinic for treatment of PC include sipuleucel-T (dendritic cell–based vaccine using prostatic acid phosphatase as antigen), Prostvac (viral-based vaccine using PSA as antigen), GVAX (whole-cell–based vaccine), tasquinimod (inhibitor of S100A9 and MDSC), and immune checkpoint inhibitors such as ipilimumab (inhibitor of CTLA-4) and pembrolizumab (inhibitor of PD-1) [25]. Results from the present study highlight heterogeneities among CRPC bone metastases that might be important to consider when choosing immunotherapy for individual PC patients. For instance, the inverse correlation between expression of MHC class I and AR-regulated genes probably diminishes response to antigen-directed vaccines targeting AR-stimulated genes (ACPP and PSA) in the majority of CRPC cases with high AR activity (Supplementary Figure 4). Instead, the high MHC class I expression, immune cell infiltration, and levels of CTLA4, PDCD1, and S100A9 observed in non–AR-driven metastases suggest testing of immune checkpoint inhibitors and Tasquinimod specifically in this subgroup of patients. However, the current study includes a limited number of clinical CRPC bone metastases, so the subgroup of 20% non–AR-driven cases is particularly small. The results need to be verified in larger cohorts, preferably including patients in trials for evaluation of immune-strengthening therapies. Therapy-predicting markers in addition to low serum PSA levels could be MHC class I expression in tumor cells and the immune cell profile in metastasis tissue and blood. In patients with multimetastatic disease, several metastases should be studied for optimal information.

The molecular drivers behind the subgroups of CRPC bone metastases observed are not known and need to be examined further. We observed high levels of the AR co-regulators FOXA1 and HOXB13, which might be responsible for programming the AR cistrome in AR-driven bone metastases [26], while the function of the prostate-derived Ets factor SPDEF in PC is more controversial [27,28]. The low immune-cell infiltration observed in AR-driven metastases might be explained in part by low levels of LYVE1 (Supplementary Table 4) and thus low predicted numbers of lymphatic vessels, recently demonstrated as a critical determinant of the metastatic process in colorectal cancer through reduced immune cytotoxicity [29]. Low levels of the monocyte/lymphocyte chemoattractant CCL5 and predicted low levels of pro-inflammatory cytokines such as IFNG, TNF, CSF2, NFKB, and IL4 could obviously contribute as well. In non–AR-driven metastases, the predicted activity of TGFβ1, IL5, and other anti-inflammatory factors might inhibit T-cell activity, possibly via activation of Tregs and MDSC as discussed above (Supplementary Table 4). The reduced expression of MHC class I antigen–processing molecules in clinical PC might be caused by structural defects, or possibly by epigenetic, transcriptional, or post-transcriptional regulation [30]. If so, there might be a possibility of restoring MHC class I expression with IFNG or drugs inhibiting methylation or histone deacetylation [11,31,32]. The inverse correlation observed between MHC class I expression and AR activity is in line with previous results showing increased lymphocyte density in human prostate after ADT [33,34] and with the general effects of androgens in suppressing both adaptive and innate immune responses [35]. Taken together, these findings support the rationale for treating PC patients with combinations of ADT and immunotherapy [36].

5. Conclusions

In conclusion, the majority of CRPC bone metastases show high AR activity, high metabolic activity, low MHC class I expression and low numbers of infiltrating immune cells. By contrast, a subgroup of metastases shows low AR and metabolic activity, but high MHC class I expression and immune cell infiltration. Targeted therapies for these two CRPC subgroups should be explored.

Author contributions: Pernilla Wikström had full access to all the data in the study and takes responsibility for the integrity of the data and the accuracy of the data analysis.

Study concept and design: Wikström.
Acquisition of data: Bovinder Ylitalo, Egevad, Bergh, Wikström.
Analysis and interpretation of data: Bovinder Ylitalo, Thysell, Lundholm, Wikström.
Drafting of the manuscript: Wikström.
Critical revision of the manuscript for important intellectual content: Bovinder Ylitalo, Thysell, Jernberg, Lundholm, Crnalic, Egevad, Stattin, Widmark, Bergh.
Statistical analysis: Thysell, Wikström.
Obtaining funding: Wikström.
Administrative, technical, or material support: Jernberg, Crnalic, Stattin, Widmark, Bergh.
Supervision: None.
Other: None.

Please cite this article in press as: Ylitalo EB, et al. Subgroups of Castration-resistant Prostate Cancer Bone Metastases Defined Through an Inverse Relationship Between Androgen Receptor Activity and Immune Response. Eur Urol (2016), http://dx.doi.org/10.1016/j.eururo.2016.07.033

Financial disclosures: Pernilla Wikström certifies that all conflicts of interest, including specific financial interests and relationships and affiliations relevant to the subject matter or materials discussed in the manuscript (eg, employment/affiliation, grants or funding, consultancies, honoraria, stock ownership or options, expert testimony, royalties, or patents filed, received, or pending), are the following: None.

Funding/Support and role of the sponsor: This study was supported by grants from Swedish Research Council (K2013-64X-20407-04-3), the Swedish Cancer Society (CAN 2013/845 and CAN 2013/1324), The Swedish Foundation for Strategic Research (RB13-0119), Cancer Research Foundation in Northern Sweden, Umeå University, the county of Västerbotten, and the Erling-Persson Family Foundation. The sponsors played no direct role in the study.

Acknowledgments: The authors are grateful to Pernilla Andersson and Susanne Gidlund for excellent technical assistance.

Appendix A. Supplementary data

Supplementary data associated with this article can be found, in the online version, at http://dx.doi.org/10.1016/j.eururo.2016.07.033.

References

[1] Nelson PS. Molecular states underlying androgen receptor activation: a framework for therapeutics targeting androgen signaling in prostate cancer. J Clin Oncol 2012;30:644–6.
[2] Omlin A, Pezaro C, Gillessen Sommer S. Sequential use of novel therapeutics in advanced prostate cancer following docetaxel chemotherapy. Ther Adv Urol 2014;6:3–14.
[3] Hörnberg E, Ylitalo EB, Crnalic S, et al. Expression of androgen receptor splice variants in prostate cancer bone metastases is associated with castration-resistance and short survival. PLoS One 2011;6:e19059.
[4] Antonarakis ES, Lu C, Wang H, et al. AR-V7 and resistance to enzalutamide and abiraterone in prostate cancer. N Engl J Med 2014;371:1028–38.
[5] Jernberg E, Thysell E, Bovinder Ylitalo E, et al. Characterization of prostate cancer bone metastases according to expression levels of steroidogenic enzymes and androgen receptor splice variants. PLoS One 2013;8:e77407.
[6] Crnalic S, Hörnberg E, Wikström P, et al. Nuclear androgen receptor staining in bone metastases is related to a poor outcome in prostate cancer patients. Endocr Relat Cancer 2010;17:885–95.
[7] Hammarsten P, Karalija A, Josefsson A, et al. Low levels of phosphorylated epidermal growth factor receptor in nonmalignant and malignant prostate tissue predict favorable outcome in prostate cancer patients. Clin Cancer Res 2010;16:1245–55.
[8] Eriksson L, Antti H, Gottfries J, et al. Using chemometrics for navigating in the large data sets of genomics, proteomics, and metabonomics (gpm). Anal Bioanal Chem 2004;380:419–29.
[9] Blades RA, Keating PJ, McWilliam LJ, George NJ, Stern PL. Loss of HLA class I expression in prostate cancer: implications for immunotherapy. Urology 1995;46:681–6.
[10] Seliger B, Stoehr R, Handke D, et al. Association of HLA class I antigen abnormalities with disease progression and early recurrence in prostate cancer. Cancer Immunol Immunother 2010;59:529–40.
[11] Kitamura H, Torigoe T, Asanuma H, Honma I, Sato N, Tsukamoto T. Down-regulation of HLA class I antigens in prostate cancer tissues and up-regulation by histone deacetylase inhibition. J Urol 2007;178:692–6.
[12] Domingo-Domenech J, Vidal SJ, Rodriguez-Bravo V, et al. Suppression of acquired docetaxel resistance in prostate cancer through depletion of notch- and hedgehog-dependent tumor-initiating cells. Cancer Cell 2012;22:373–88.
[13] Thysell E, Surowiec I, Hörnberg E, et al. Metabolomic characterization of human prostate cancer bone metastases reveals increased levels of cholesterol. PLoS One 2010;5:e14175.
[14] Iglesias-Gato D, Wikström P, Tyanova S, et al. The proteome of primary prostate cancer. Eur Urol 2016;69:942–52.
[15] Mahoney KM, Rennert PD, Freeman GJ. Combination cancer immunotherapy and new immunomodulatory targets. Nat Rev Drug Discov 2015;14:561–84.
[16] Marchesi M, Andersson E, Villabona L, et al. HLA-dependent tumour development: a role for tumour associate macrophages? J Transl Med 2013;11:247.
[17] Strasner A, Karin M. Immune Infiltration and Prostate Cancer. Front Oncol 2015;5:128.
[18] Davidsson S, Ohlson AL, Andersson SO, et al. CD4 helper T cells, CD8 cytotoxic T cells, and FOXP3$^+$ regulatory T cells with respect to lethal prostate cancer. Mod Pathol 2013;26:448–55.
[19] Flammiger A, Weisbach L, Huland H, et al. High tissue density of FOXP3$^+$ T cells is associated with clinical outcome in prostate cancer. Eur J Cancer 2013;49:1273–9.
[20] Lanciotti M, Masieri L, Raspollini MR, et al. The role of M1 and M2 macrophages in prostate cancer in relation to extracapsular tumor extension and biochemical recurrence after radical prostatectomy. BioMed Res Int 2014;2014:486798.
[21] Tidehag V, Hammarsten P, Egevad L, et al. High density of S100A9 positive inflammatory cells in prostate cancer stroma is associated with poor outcome. Eur J Cancer 2014;50:1829–35.
[22] Lundholm M, Hägglöf C, Wikberg ML, et al. Secreted factors from colorectal and prostate cancer cells skew the immune response in opposite directions. Sci Rep 2015;5:15651.
[23] Idorn M, Kollgaard T, Kongsted P, Sengelov L, Thor Straten P. Correlation between frequencies of blood monocytic myeloid-derived suppressor cells, regulatory T cells and negative prognostic markers in patients with castration-resistant metastatic prostate cancer. Cancer Immunol Immunother 2014;63:1177–87.
[24] Wang L, Gong Y, Chippada-Venkata U, et al. A robust blood gene expression-based prognostic model for castration-resistant prostate cancer. BMC Med 2015;13:201.
[25] Saad F, Miller K. Current and emerging immunotherapies for castration-resistant prostate cancer. Urology 2015;85:976–86.
[26] Pomerantz MM, Li F, Takeda DY, et al. The androgen receptor cistrome is extensively reprogrammed in human prostate tumorigenesis. Nat Genet 2015;47:1346–51.
[27] Cheng XH, Black M, Ustiyan V, et al. SPDEF inhibits prostate carcinogenesis by disrupting a positive feedback loop in regulation of the Foxm1 oncogene. PLoS Genet 2014;10:e1004656.
[28] Kim IJ, Kang TW, Jeong T, Kim YR, Jung C. HOXB13 regulates the prostate-derived Ets factor: implications for prostate cancer cell invasion. Int J Oncol 2014;45:869–76.
[29] Mlecnik B, Bindea G, Kirilovsky A, et al. The tumor microenvironment and immunoscore are critical determinants of dissemination to distant metastasis. Sci Transl Med 2016;8, 327ra26.
[30] Bukur J, Jasinski S, Seliger B. The role of classical and non-classical HLA class I antigens in human tumors. Semin Cancer Biol 2012;22:350–8.
[31] Chang CC, Pirozzi G, Wen SH, et al. Multiple structural and epigenetic defects in the human leukocyte antigen class I antigen presentation pathway in a recurrent metastatic melanoma following immunotherapy. J Biol Chem 2015;290:26562–75.
[32] Fonsatti E, Nicolay HJ, Sigalotti L, et al. Functional up-regulation of human leukocyte antigen class I antigens expression by 5-aza-2′-

deoxycytidine in cutaneous melanoma: immunotherapeutic implications. Clin Cancer Res 2007;13:3333–8.

[33] Gannon PO, Poisson AO, Delvoye N, Lapointe R, Mes-Masson AM, Saad F. Characterization of the intra-prostatic immune cell infiltration in androgen-deprived prostate cancer patients. J Immunol Methods 2009;348:9–17.

[34] Sorrentino C, Musiani P, Pompa P, Cipollone G, Di Carlo E. Androgen deprivation boosts prostatic infiltration of cytotoxic and regulatory T lymphocytes and has no effect on disease-free survival in prostate cancer patients. Clin Cancer Res 2011;17:1571–81.

[35] Trigunaite A, Dimo J, Jorgensen TN. Suppressive effects of androgens on the immune system. Cell Immunol 2015;294:87–94.

[36] Drake CG, Sharma P, Gerritsen W. Metastatic castration-resistant prostate cancer: new therapies, novel combination strategies and implications for immunotherapy. Oncogene 2014;33:5053–64.

Please cite this article in press as: Ylitalo EB, et al. Subgroups of Castration-resistant Prostate Cancer Bone Metastases Defined Through an Inverse Relationship Between Androgen Receptor Activity and Immune Response. Eur Urol (2016), http://dx.doi.org/10.1016/j.eururo.2016.07.033